

Published in final edited form as:

Science. 2015 November 20; 350(6263): 928–932. doi:10.1126/science.aad0843.

Stable recombination hotspots in birds

Sonal Singhal^{*,1,2,+}, Ellen M. Leffler^{*,3,4}, Keerthi Sannareddy³, Isaac Turner⁴, Oliver Venn⁴, Daniel M. Hooper⁵, Alva I. Strand¹, Qiye Li⁶, Brian Raney⁷, Christopher N. Balakrishnan⁸, Simon C. Griffith⁹, Gil McVean⁴, and Molly Przeworski^{1,2,+}

¹Columbia University, Dept. of Biological Sciences, New York, NY

²Columbia University, Dept. of Systems Biology, New York, NY

³University of Chicago, Dept. of Human Genetics, Chicago, IL

⁴University of Oxford, Wellcome Trust Centre for Human Genetics, Oxford, United Kingdom

⁵Committee on Evolutionary Biology, University of Chicago, Chicago, IL

⁶China National GeneBank, BGI-Shenzhen, China

⁷University of California Santa Cruz, Center for Biomolecular Science & Engineering, Santa Cruz, CA

⁸East Carolina University, Biology, Greenville, NC

⁹Macquarie University, Dept. of Biological Sciences, Sydney, Australia

Abstract

The DNA-binding protein PRDM9 has a critical role in specifying meiotic recombination hotspots in mice and apes, but appears to be absent from other vertebrate species, including birds. To study the evolution and determinants of recombination in species lacking *PRDM9*, we inferred fine-scale genetic maps from population resequencing data for two bird species, the zebra finch *Taeniopygia guttata* and the long-tailed finch *Poephila acuticauda*. We find that both species have hotspots, which are enriched near functional genomic elements. Unlike in mice and apes, the two species share most hotspots, with conservation seemingly extending over tens of millions of years. These observations suggest that in the absence of PRDM9, recombination targets functional features that both enable access to the genome and constrain its evolution.

Meiotic recombination is a ubiquitous and fundamental genetic process that shapes variation in populations, yet our understanding of its underlying mechanisms is based on a handful of model organisms, scattered throughout the tree of life. One pattern shared among most sexually reproducing species is that meiotic recombination tends to occur in short segments of 100s to 1000s of base pairs, termed “recombination hotspots” (1). In apes and mice, the location of hotspots is largely determined by PRDM9, a zinc-finger protein that binds to specific motifs in the genome during meiotic prophase and generates H3K4me3 marks, eventually leading to double-strand breaks (DSBs) and both crossover and non-crossover

⁺to whom correspondence should be addressed.

^{*}co-first authors

resolutions (2–5). In mammals, the zinc-finger domain of *PRDM9* evolves quickly, with evidence of positive selection on residues in contact with DNA (2, 6), and as a result, there is rapid turnover of hotspot locations across species, subspecies, and populations (7–10).

Although *PRDM9* plays a pivotal role in controlling recombination localization in mice and apes, many species lacking *PRDM9* nonetheless have hotspots (6). An artificial example is provided by mice knockouts for *PRDM9*. Despite being sterile, they make similar numbers of DSBs as wild-type mice, and their recombination hotspots appear to default to residual H3K4me3 mark locations, notably at promoters (10). A natural but puzzling example is provided by canids, which carry premature stop codons in *PRDM9* yet are able to recombine and remain fertile (11, 12). Like in mouse *PRDM9* knockouts, in dogs and in other species without *PRDM9* such as the yeast *Saccharomyces cerevisiae* and the plant *Arabidopsis thaliana*, hotspots tend to occur at promoters or other regions with promoter-like features (11, 13, 14). In yet other taxa without *PRDM9*, including *Drosophila* species (15), honeybees (16), and *Caenorhabditis elegans* (17), short, intense recombination hotspots appear to be absent altogether.

To further explore how the absence of *PRDM9* shapes the fine-scale recombination landscape and impacts its evolution, we turn to birds, because an analysis of the chicken genome suggested that it may not have *PRDM9* (6). We first confirmed the absence of *PRDM9* across reptiles by querying the genomes of 48 species of birds, three species of crocodylians, two species of turtles, and one species of lizard for *PRDM9* (18), finding that only the turtle genomes contain putative orthologs with all three *PRDM9* domains (Fig. S1). We also found no expression of any *PRDM9*-like transcripts in RNAseq data from testes tissue of the zebra finch (*Taeniopygia guttata*) (18). Given the likely absence of *PRDM9* in birds, we ask: is recombination nonetheless concentrated in hotspots in these species? If so, how quickly do the hotspots evolve? Where does recombination tend to occur in the genome? To address these questions, we generated whole-genome resequencing data for wild populations from two bird species and inferred fine-scale genetic maps from patterns of linkage disequilibrium.

Inferring fine-scale recombination maps

We sampled three species of finch in the family *Estrildidae*: zebra finch (*Taeniopygia guttata*; n=19 wild, unrelated birds and n=5 from a domesticated, nuclear family), long-tailed finch (*Poephila acuticauda*; n=20, including 10 of each of two, similar subspecies with average autosomal $F_{ST} = 0.039$), and, for use as an outgroup, double-barred finch (*Taeniopygia bichenovii*; n=1) [Fig. 1, Table S1; (18)]. Despite extensive incomplete lineage sorting between the species, they do not appear to have diverged with gene flow (Fig. S2). Moreover, nucleotide divergence among the three finch species is similar to that of human, chimpanzee and gorilla, providing a well-matched comparison to apes (8, 9) (Fig. 1).

We mapped reads from all individuals to the zebra finch reference genome [1 Gb assembled across 34 chromosomes; (19)] and generated *de novo* SNP calls for all three species. After filtering for quality, we identified 44.6 million SNPs in zebra finch, 26.2 million SNPs in long-tailed finch, and 3.0 million SNPs in double-barred finch (Table S2). These SNP

numbers correspond to autosomal nucleotide diversity of $\pi=0.82\%$ and $\theta_w=1.37\%$ in zebra finch and $\pi=0.55\%$ and $\theta_w=0.73\%$ in long-tailed finch, approximately ten times higher than estimates in apes (20). Assuming a mutation rate per base pair per generation of 7×10^{-10} (18), these diversity levels suggest a long-term effective population size (N_e) of 4.8×10^6 and 2.5×10^6 in the zebra finch and long-tailed finch, respectively. Thus, these two species have much larger N_e than most other species for which there exist fine-scale recombination maps, with N_e more reflective of biodiversity at large (Fig. S3).

Next, we inferred haplotypes for zebra finch and long-tailed finch using a linkage-disequilibrium approach that incorporated phase-informative reads and family phasing. From the haplotypes, we estimated fine-scale recombination maps using LDhelmet, which works well for species with higher nucleotide diversity (15). The resulting maps estimated median recombination rates in the zebra finch and long-tailed finch genomes as $\rho = 26.2/\text{kb}$ and $14.0/\text{kb}$, respectively, which corresponds to a median rate of 0.14 cM/Mb in both species (18). Simulations indicated that we had limited power to identify hotspots in regions with high recombination rates (Fig. S4), so we restricted our analyses to the 18 largest chromosomes in the reference genome (930 Mb; 91% of the assembled genome). For these 18 chromosomes, our results accord well with recombination maps inferred from a more limited pedigree-based study of zebra finch (21), with a correlation of 0.90 for rates estimated at the 5 Mb scale (Fig. S5), providing confidence in our rate inferences.

Hotspots and their evolution

To identify hotspots in the genome, we operationally define them as regions that are at least 2 kb in length, have at least 5-fold the background recombination rate as estimated across the 80 kb of sequence surrounding the region, and are statistically supported as hotspots by a likelihood ratio test (18). This approach yielded 3949 hotspots in zebra finch and 4933 hotspots in long-tailed finch (Figs. 2, S6, S7), with one hotspot detected on average every 215 and 179 kb in the two species, respectively. Both the lower density of hotspots in zebra finch than in long-tailed finch and the lower density of hotspots in the finches compared to humans is consistent with simulations that indicate decreased power to detect hotspots when the background population recombination rate is higher (18, Figs. S4, S8). Importantly, the hotspots were detected after aggressively filtering our SNP datasets and show no evidence of having higher phasing error rates than the rest of the genome (Table S3, S4, Fig. S9).

Considering hotspots as shared if their midpoints occur within 3 kb of each other, 73% of zebra finch hotspots (2874 of 3949 hotspots) were detected as shared between the two species (Fig. S10) when only 4.4% were expected to overlap by chance (Figs. S10, 11); similar results were obtained under different criteria for hotspot sharing (Table S5). The true fraction of shared hotspots between zebra finch and long-tailed finch is likely higher than observed, because we do not have complete power (Fig. S4) and simulations suggest that we are unlikely to detect spurious cases of hotspot sharing (18). On the other hand, the observed levels of sharing are somewhat lower than expected compared to a model in which all hotspots are identical in the two species (Fig. S12).

This conservation of hotspots contrasts sharply with comparative analyses in apes and mice, where, even across populations with modest levels of genetic differentiation, there is no hotspot sharing (8–10). In fact, if we apply the same criterion for hotspot sharing to humans and chimpanzees, only 10.5% of chimpanzee hotspots overlap with human hotspots when a 7.2% overlap is expected by chance (Fig. S11).

To provide further support for the validity of the inferred hotspots, we tested if they show evidence for GC-biased gene conversion (gBGC), measured as higher expected equilibrium levels of GC content (GC*; 18). Because evidence for gBGC in birds is somewhat indirect (22), we first looked for support for gBGC at broad genomic scales, finding a positive relationship between recombination rate and GC* (Fig. 3A-B). Narrowing our focus to the regions surrounding hotspots, we observe that hotspots exhibit peaked GC* relative to both flanking sequence and coldspots (i.e., regions without peaks in recombination) matched for the same overall GC and CpG content (Fig. 4A-B). A similar phenomenon is seen in intra-species variation data: at hotspots but not matched coldspots, derived alleles segregate at a higher frequency at AT to GC polymorphisms than at GC to AT polymorphisms (Fig. S13). Thus, two independent signatures of recombination—patterns of linkage disequilibrium and of base composition—converge in demonstrating that finches have recombination hotspots and that these are conserved over much larger time scales than in apes and mice (8–10).

After observing the pattern of gBGC at hotspots in zebra finch and long-tailed finch, we tested how far conservation of hotspot locations extends across the avian phylogeny by additionally considering the genomes of double-barred finch (an estimated ~3.5 million years [myr] from zebra finch (18)), medium ground finch *Geospiza fortis* (~15.5 myr from zebra finch (23)), and collared flycatcher *Ficedula albicollis* (~19.1 myr from zebra finch (24)). Because we only had a single diploid genome from these species, we tested for hotspot conservation indirectly by determining if these species had peaks in GC* at the hotspot locations inferred as shared between zebra finch and long-tailed finch. We find localized GC* peaks at hotspots in all three species (Fig. 4C-E), suggesting that the conservation of hotspots extends across tens of millions of years of evolution. Intriguingly, these findings echo those obtained from four species of *Saccharomyces* yeast, which show nearly complete conservation of hotspot locations and intensities across species 15 myr diverged (25). Almost all hotspots in *Saccharomyces* yeast occur at promoters, which are evolutionarily stable, suggesting that how hotspot locations are specified influences how they evolve (12, 26).

The localization of hotspots in the genome

Hotspots in zebra finch and long-tailed finch are enriched near transcription start sites (TSSs), transcription stop sites (TESs) and CpG islands (CGIs), with close to half of all hotspots occurring within 3 kb of one of these features (~17% occur within 3 kb of both an annotated TSS and CGI, 3% within 3 kb of both a TES and CGI, and ~26% within 3 kb of a CGI only; Fig. S14). In particular, the hotspots near CGIs are more likely to be shared between species and exhibit stronger evidence for gBGC compared to hotspots distant from CGIs (Fig. S15), providing further support for the importance of these elements in the targeting of recombination. Consistent with the findings about hotspots, recombination rates

are nearly two-fold higher near annotated TSSs and TESs (Fig. 5A-B). This pattern appears to be driven mainly by their co-localization with CGIs (Fig. 5A-B, Fig. S16): rates near CGIs are more than three-fold higher with only a small further increase if they are near a TSS or a TES (Fig. 5C-D; Fig. S17).

A positive association between proximity to the TSS and recombination rate has been previously reported in a number of species without *PRDM9*, including *S. cerevisiae*, the monkey-flower *Mimulus guttatus*, dogs, and *A. thaliana* (11, 13, 14, 27) and an association between TES and recombination rate has been shown in *A. thaliana* (14). In turn, the link between CGIs and recombination rates has been found both in species without *PRDM9* including dogs (11) and, albeit more weakly, in species with *PRDM9* including humans and chimpanzees (9). Moreover, the relationship between distance to CGIs and recombination rate remains significant after controlling for expression levels in zebra finch testes (Spearman's $r=-0.11$; $p=4.32 \times 10^{-27}$, Fig. S18). This increase in recombination rates near TSSs, TESs and CGIs supports a model in which, particularly in the absence of *PRDM9* binding specificity, recombination is concentrated at functional elements that are accessible to the recombination machinery. Indeed, all three coincide with destabilization of nearby nucleosome occupancy (28, 29) and both TSSs and CGIs serve as sites of transcription initiation (30). An intriguing implication is that the structure of linkage disequilibrium may differ systematically between species with and without *PRDM9*, with tighter coupling between regulatory and exonic variants in species with *PRDM9*.

Under a model in which the recombination machinery tends to target accessible genomic elements, we would not necessarily expect to see enrichment of specific binding motifs associated with hotspot activity. Accordingly then, when we test for motifs enriched in hotspots relative to coldspots, the top motifs in both species are a string of As, which are also enriched in *A. thaliana* and yeast hotspots and which may be nucleosome depleted or facilitate nucleosome removal (13, 31) (Fig. S19). We also find a number of additional motifs that are GC-rich and perhaps indicative of CGIs.

At even finer resolution, recombination rates are higher in exonic than intronic regions, which has also been seen in *A. thaliana* (14), dogs (11), and *M. guttatus* (27) and higher towards the ends of the gene than in the middle (Fig. 5E-F). One possibility for these patterns is that DSBs preferentially initiate in exons near the TSS and TES and their resolution occurs in intervening exons and introns. The specific mechanism by which DSBs would preferentially initiate in exons is unknown, but the pattern is consistent with an important role for chromatin marks that distinguish exons from introns (28).

Contrasting tempos of broad- and fine scale recombination rate evolution

Median recombination rates across and within chromosomes vary over nearly six orders of magnitude (Figs. S8, S20), creating a heterogeneous landscape of broad-scale recombination rates across the genome, with regions of elevated recombination near telomeres and large intervening deserts (as found in zebra finch pedigree data; (21)). Indeed, most of the recombination events in zebra finch and long-tailed finch occur in a narrow portion of the genome, with 82% and 70% of events localized to 20% of the genome in zebra finch and

long-tailed finch, respectively (Fig. S21). Notably, recombination rates for the Z sex chromosome are two orders of magnitude lower than the most similarly sized autosome, chromosome 1A, even after accounting for the lack of recombination in females (Fig. S8, (21)). Although cytological data indicate that both zebra finch and long-tailed finch harbor a pericentric inversion polymorphism over much of chromosome Z (32, 33), such an inversion is unlikely to explain this extreme a difference (18).

Between zebra finch and long-tailed finch, broad-scale rates are highly similar, with genome-wide correlations of 0.82 and 0.86 at the 10 kb and 1 Mb scales, respectively (Figs. 6, S20). Despite this broad-scale concordance, we infer that some genomic regions between the two species have very different rates of recombination (Fig. S22) and find tentative support for some of these changes in the derived allele frequency spectra (Fig. S23). Moreover, at a greater evolutionary distance, broad-scale patterns differ markedly; the collared flycatcher (~19 myr diverged) has a relatively homogeneous recombination landscape compared to zebra finch and long-tailed finch (24). This evolution of broad-scale rates is particularly notable because, in many species, shifts in broad-scale recombination patterns can be explained almost entirely by chromosomal rearrangements, shifts in karyotypes, and changes in chromosome lengths (9, 34, 35). However, there is no obvious pattern by which chromosomal rearrangements drive differences in recombination rates between zebra finch and long-tailed finch (Fig. S22), and, despite harboring a number of small inversions between them, collared flycatcher and zebra finch have similar karyotypes and syntenic genomes (24). That broad-scale recombination patterns have changed across the same phylogenetic breadth for which we see hotspot conservation suggests two non-exclusive possibilities that merit further investigation: either the heats or locations of some hotspots have evolved, or rates have changed in regions that fall outside of our operational definition of hotspots.

The impact of recombination on the genome

Given the marked variation in recombination rates across the genome, we consider the consequences for genome evolution. First, we note that increased recombination rates drive increasing GC content in the genome, presumably via gBGC, and we see this phenomenon both at the genome-wide scale (Fig. 3A-B) and the scale of hotspots (Fig. 4). An extreme example is provided by the pseudoautosomal region (PAR), which we identified on an unassembled scaffold from chromosome Z using estimates of coverage in males and females. We confirmed the PAR by inferring homology to PARs identified in medium ground finch and collared flycatcher (Fig. S24). The PAR is short—estimated to be just 450 kb—and is subject to an obligate crossover in every female meiosis (36); as such, it has very high recombination rates. The consequence is visible in the high GC* for the PAR, which exceeds estimates of GC* across most of the rest of chromosome Z in both species (Fig. 3C-D).

Further, as has been reported for many other organisms, including chickens (37–39), our results suggest that recombination is positively correlated with levels of nucleotide diversity, particularly on the Z (Fig. S25–27). This observation is consistent with widespread effects of linked selection in these species (40).

Conclusion

Finches lack PRDM9 yet nonetheless harbor hotspots, with recombination concentrated at functional elements (TESs, TSSs, and CGIs) that likely denote greater accessibility to the cellular recombination machinery. In sharp contrast to apes and mice, the hotspot locations are conserved among species several millions of years diverged and likely over tens of millions of years. These results suggest that the genetic architecture of recombination influences the rate at which hotspots evolve. Whereas the binding specificity of PRDM9 drives rapid turnover, the reliance on accessible, functional genomic features leads to stasis. This hypothesis accords with recent results in yeast, in which recombination is concentrated at promoters, and hotspots are stable in intensity and location over tens of millions of years (25). To further investigate how deeply this stasis extends and explore the taxonomic generality of these findings, the approaches illustrated here can be applied to other sequenced bird species (41) and beyond. In doing so, we will begin to better understand why species differ so drastically in their specification of hotspots and, in particular, why a subset rely on PRDM9.

Supplementary Materials

Refer to Web version on PubMed Central for supplementary material.

Acknowledgements

This project was started when MP was a Howard Hughes Medical Institute Early Career Scientist and was funded, in part, by Wellcome Trust grants 086786/Z/08/Z to O.V. and 090532/Z/09/Z to the Wellcome Trust Centre for Human Genetics. We thank B. de Massy, C. Grey, S. Myers, T. Price, M. Schumer, J. Wall, A. Williams and J. Willis for helpful discussions and/or comments on the manuscript; K. Argoud and P. Piazza at the Genomics Core at the Wellcome Trust Centre for Human Genetics for assistance with lab work; and M. T. Gilbert for sharing the zebra finch gene annotations in advance of publication. We thank I. Lam and S. Keeney for sharing their unpublished manuscript with us, and S. Keeney for many helpful discussions. BAM alignment files for genomic data and filtered variant call files (VCFs) for zebra finch, long-tailed finch, and double-barred finch are available at <http://www.ebi.ac.uk/ena/data/view/PRJEB10586>. Sequence reads for RNAseq experiments in zebra finch are available at <http://www.ncbi.nlm.nih.gov/bioproject/?term=PRJNA295077>. Masked genome files, the reconstructed ancestral genome, and recombination maps for both species are available at DataDryad: doi:10.5061/dryad.fd24j. All scripts and an electronic lab notebook for this work are available at <https://github.com/singhal/postdoc> and <https://github.com/singhal/labnotebook>, respectively.

References and Notes

1. de Massy B. Annual review of genetics. 2013; 47:563.
2. Myers S, et al. Science. 2010; 327:876. [PubMed: 20044541]
3. Berg IL, et al. Nature genetics. 2010; 42:859. [PubMed: 20818382]
4. Baudat F, et al. Science. 2010; 327:836. [PubMed: 20044539]
5. Williams AL, et al. eLife. 2015; 4:e04637.
6. Oliver PL, et al. PLoS Genet. 2009; 5:e1000753. [PubMed: 19997497]
7. Hinch AG, et al. Nature. 2011; 476:170. [PubMed: 21775986]
8. Stevison LS, et al. bioRxiv. 2015:013755.
9. Auton A, et al. Science. 2012; 336:193. [PubMed: 22422862]
10. Brick K, Smagulova F, Khil P, Camerini-Otero RD, Petukhova GV. Nature. 2012; 485:642. [PubMed: 22660327]
11. Auton A, et al. PLoS Genetics. 2013; 9
12. Axelsson E, et al. Genome research. 2012; 22:51. [PubMed: 22006216]

13. Pan J, et al. *Cell*. 2011; 144:719. [PubMed: 21376234]
14. Choi K, et al. *Nature genetics*. 2013; 45:1327. [PubMed: 24056716]
15. Chan AH, Jenkins PA, Song YS. *PLoS genetics*. 2012; 8:e1003090. [PubMed: 23284288]
16. Wallberg A, Gle´min S, Webster MT. *PLoS Genetics*. 2015; 11
17. Kaur T, Rockman MV. *Genetics*. 2014; 196:137. [PubMed: 24172135]
18. Materials and methods are available as supplementary materials on Science Online.
19. Warren WC, et al. *Nature*. 2010; 464:757. [PubMed: 20360741]
20. Leffler EM, et al. *PLoS Biol*. 2012; 10:e1001388. [PubMed: 22984349]
21. Backstrom N, et al. *Genome research*. 2010; 20:485. [PubMed: 20357052]
22. Weber CC, Boussau B, Romiguier J, Jarvis ED, Ellegren H. *Genome biology*. 2014; 15:549. [PubMed: 25496599]
23. Zhang G, Parker P, Li B, Li H, Wang J. *GigaScience*. 2012; 1:13. [PubMed: 23587407]
24. Kawakami T, et al. *Molecular ecology*. 2014; 23:4035. [PubMed: 24863701]
25. Lam I, Keeney S. *bioRxiv*. 2015:023176.
26. Nicolas A, Treco D, Schultes NP, Szostak JW. *Nature*. 1989; 338:35. [PubMed: 2537472]
27. Hellsten U, et al. *Proceedings of the National Academy of Sciences*. 2013; 110:19478.
28. Jones PA. *Nature Reviews Genetics*. 2012; 13:484.
29. Kaplan N, et al. *Nature*. 2009; 458:362. [PubMed: 19092803]
30. Deaton AM, Bird A. *Genes & development*. 2011; 25:1010. [PubMed: 21576262]
31. Wijnker E, et al. *Elife*. 2013; 2:e01426. [PubMed: 24347547]
32. Christidis L. *Genetica*. 1986; 71:81.
33. Itoh Y, Kampf K, Balakrishnan CN, Arnold AP. *Chromosoma*. 2011; 120:255. [PubMed: 21369954]
34. Dumont BL, Payseur BA. *Evolution*. 2008; 62:276. [PubMed: 18067567]
35. Jensen-Seaman MI, et al. *Genome research*. 2004; 14:528. [PubMed: 15059993]
36. Otto SP, et al. *Trends in Genetics*. 2011; 27:358. [PubMed: 21962971]
37. Nachman MW. *TRENDS in Genetics*. 2001; 17:481. [PubMed: 11525814]
38. Begun DJ, Aquadro CF. *Nature*. 1992; 356:519. [PubMed: 1560824]
39. Mugal CF, Arndt PF, Ellegren H. *Molecular Biology and Evolution*. 2013; 30:1700. [PubMed: 23564940]
40. Charlesworth B, Morgan M, Charlesworth D. *Genetics*. 1993; 134:1289. [PubMed: 8375663]
41. Zhang G, et al. *Science*. 2014; 346:1311. [PubMed: 25504712]
42. Griffith SC, Pryke SR, Mariette M. *Emu*. 2009; 108:311.
43. Rollins LA, Svedin N, Pryke SR, Griffith SC. *Ecology and evolution*. 2012; 2:1208. [PubMed: 22833795]
44. Pesole G, et al. *Gene*. 2001; 276:73. [PubMed: 11591473]
45. Nylander, J. *Mraic.pl*. 2004. <https://github.com/nylander/MrAIC>
46. Guindon S, et al. *Systematic biology*. 2010; 59:307. [PubMed: 20525638]
47. Liu L, Yu L, Pearl DK, Edwards SV. *Systematic Biology*. 2009; 58:468. [PubMed: 20525601]
48. Bouckaert R, et al. *PLoS Comput Biol*. 2014; 10:e1003537. [PubMed: 24722319]
49. Agate R, Scott B, Haripal B, Lois C, Nottebohm F. *PNAS*. 2009; 106:17963. [PubMed: 19815496]
50. Hooper DM, Price TD. *Evolution*. 2015; 69:890. [PubMed: 25756186]
51. Price TD, et al. *Nature*. 2014; 509:222. [PubMed: 24776798]
52. Jetz W, Thomas G, Joy J, Hartmann K, Mooers A. *Nature*. 2012; 491:444. [PubMed: 23123857]
53. Jarvis ED, et al. *Science*. 2014; 346:1320. [PubMed: 25504713]
54. Pickrell JK, Pritchard JK. *PLoS Genet*. 2012; 8:e1002967. [PubMed: 23166502]
55. Reich D, Thangaraj K, Patterson N, Price AL, Singh L. *Nature*. 2009; 461:489. [PubMed: 19779445]
56. St John JA, et al. *Genome biology*. 2012; 13:415. [PubMed: 22293439]

57. Camacho C, et al. *BMC bioinformatics*. 2009; 10:421. [PubMed: 20003500]
58. Birney E, Clamp M, Durbin R. *Genome research*. 2004; 14:988. [PubMed: 15123596]
59. Baudat F, Imai Y, de Massy B. *Nature Reviews Genetics*. 2013; 14:794.
60. Kent WJ. *Genome research*. 2002; 12:656. [PubMed: 11932250]
61. Quinlan AR, Hall IM. *Bioinformatics*. 2010; 26:841. [PubMed: 20110278]
62. McKenna A, et al. *Genome research*. 2010; 20:1297. [PubMed: 20644199]
63. Zhou Q, et al. *Science*. 2014; 346:1246338. [PubMed: 25504727]
64. Smeds L, et al. *Nature communications*. 2014; 5
65. Harris, RS. Improved pairwise alignment of genomic DNA. ProQuest; 2007.
66. Lunter G, Goodson M. *Genome research*. 2011; 21:936. [PubMed: 20980556]
67. Li H. arXiv preprint arXiv: 1303.3997. 2013
68. Iqbal Z, Caccamo M, Turner I, Flicek P, McVean G. *Nature genetics*. 2012; 44:226. [PubMed: 22231483]
69. Li H, et al. *Bioinformatics*. 2009; 25:2078. [PubMed: 19505943]
70. 1000 Genomes Project Consortium. *Nature*. 2010; 467:1061. [PubMed: 20981092]
71. Purcell S, et al. *The American Journal of Human Genetics*. 2007; 81:559. [PubMed: 17701901]
72. Pritchard JK, Przeworski M. *The American Journal of Human Genetics*. 2001; 69:1. [PubMed: 11410837]
73. Rands CM, et al. *Bmc Genomics*. 2013; 14:95. [PubMed: 23402223]
74. Langmead B, Salzberg SL. *Nature methods*. 2012; 9:357. [PubMed: 22388286]
75. Watterson G. *Theoretical population biology*. 1975; 7:256. [PubMed: 1145509]
76. Tajima F. *Genetics*. 1989; 123:597. [PubMed: 2599369]
77. Balakrishnan CN, Edwards SV. *Genetics*. 2009; 181:645. [PubMed: 19047416]
78. Williams AL, Housman DE, Rinard MC, Gifford DK. *Genome biology*. 2010; 11:R108. [PubMed: 21034477]
79. Delaneau O, Howie B, Cox AJ, Zagury JF, Marchini J. *AJHG*. 2013; 93:687.
80. Stephens M, Donnelly P. *The American Journal of Human Genetics*. 2003; 73:1162. [PubMed: 14574645]
81. Coop G, Przeworski M. *Nature Reviews Genetics*. 2007; 8:23.
82. Choi K, Henderson IR. *The Plant Journal*. 2015
83. Auton A, McVean G. *Genome research*. 2007; 17:1219. [PubMed: 17623807]
84. Chen GK, Marjoram P, Wall JD. *Genome research*. 2009; 19:136. [PubMed: 19029539]
85. Fearnhead P. *Bioinformatics*. 2006; 22:3061. [PubMed: 17060358]
86. I. H. Consortium. *Nature*. 2005; 437:1299. [PubMed: 16255080]
87. Ellegren H, et al. *Nature*. 2012; 491:756. [PubMed: 23103876]
88. Sueoka N. *PNAS*. 1962; 48:582. [PubMed: 13918161]
89. Meunier J, Duret L. *Molecular Biology and Evolution*. 2004; 21:984. [PubMed: 14963104]
90. Bailey TL, Johnson J, Grant CE, Noble WS. *Nucleic acids research*. 2015:gkv416.
91. Flicek P, et al. *Nucleic acids research*. 2011:gkr991.
92. Roberts A, Pachter L. *Nature methods*. 2013; 10:71. [PubMed: 23160280]
93. Rausch T, et al. *Bioinformatics*. 2012; 28:i333. [PubMed: 22962449]
94. Pratto F, et al. *Science*. 2014; 346:1256442. [PubMed: 25395542]

One-Sentence Summary

We show that the fine-scale recombination landscape is stable across tens of millions of years in birds, in sharp contrast to what is seen in primates and mice.

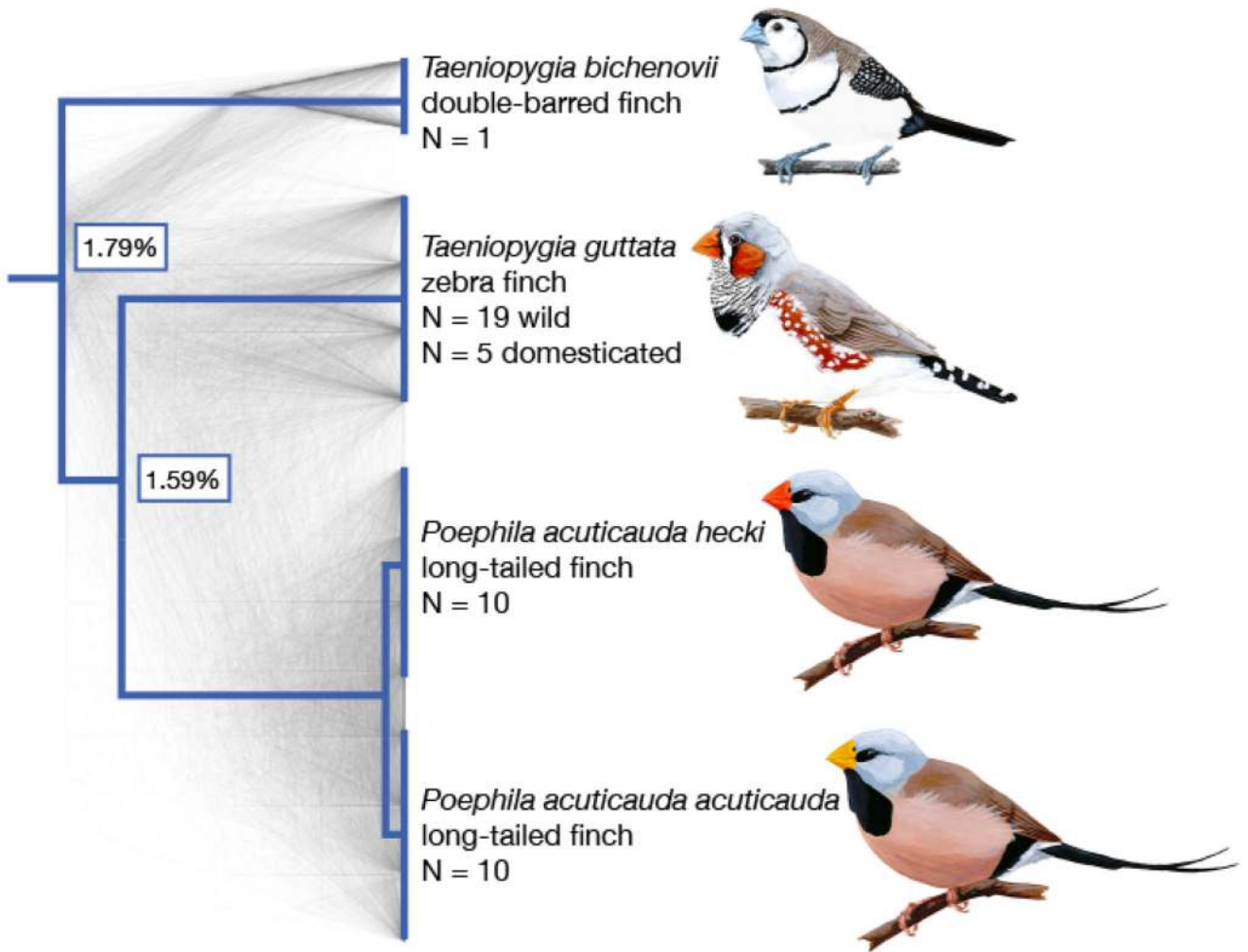


Figure 1.

Species tree for the finch species in this study. Species sampled were double-barred finch (*Taeniopygia bichenovii*), zebra finch (*T. guttata*), and the two long-tailed finch subspecies (*Poephila acuticauda hecki* and *P. a. acuticauda*). Tree rooted with medium ground finch and collared flycatcher (*Geospiza fortis* and *Ficedula albicollis*; full phylogeny shown in Fig. 4). Shown in gray are 1000 gene trees, which were used to infer the species tree (18). The pairwise divergence between species is indicated at nodes, as measured by the genome-wide average across autosomes. Images of birds from Wikimedia Commons.

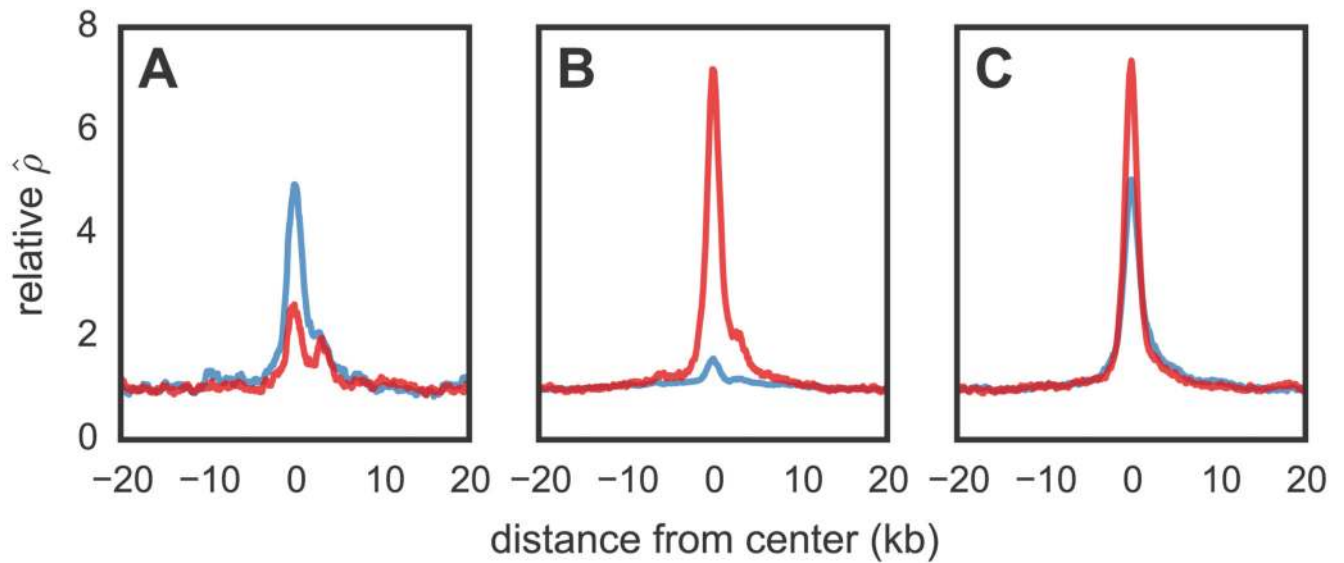


Figure 2.

Recombination rates across hotspots in zebra finch and long-tailed finch. Average relative recombination rate ($\hat{\rho}/\text{bp}$ divided by the background $\hat{\rho}$ of 20 kb on either side of the hotspot) across (A) hotspots detected only in zebra finch ($n=1075$; shown in blue), (B) those detected only in long-tailed finch (middle; $n=2059$; shown in red), and (C) those inferred as shared in the two species (right; $n=2874$). Shared hotspots are those whose midpoints occur within 3 kb of each other. The orientation of hotspots is with respect to the genomic sequence.

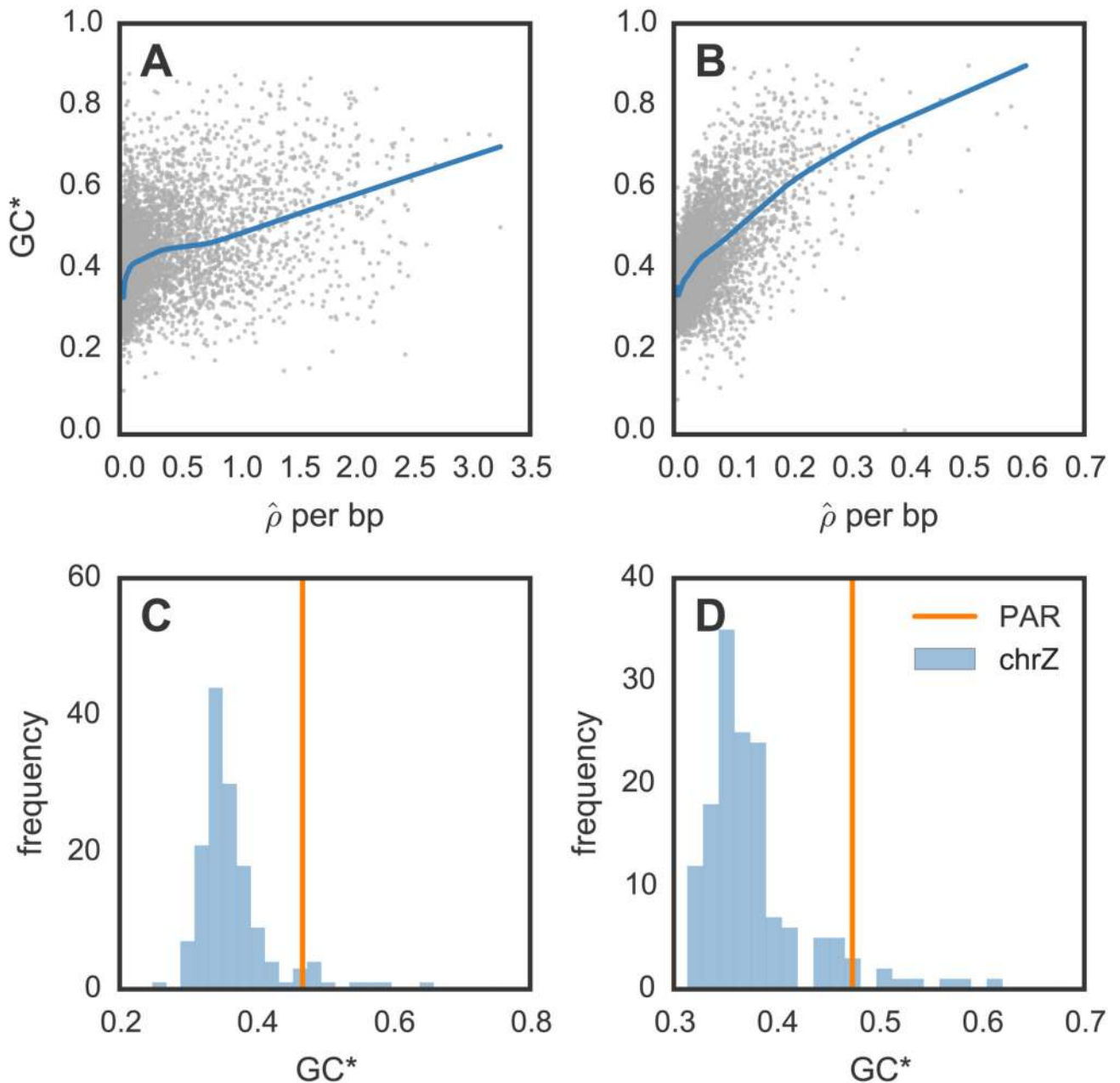


Figure 3.

Equilibrium GC content and broad-scale recombination rates in zebra finch (A, C) and long-tailed finch (B, D). (A-B) Relationship between equilibrium GC content [GC^* ; 18]) and $\hat{\rho}$ /bp for zebra finch and long-tailed finch across all autosomal chromosomes. Both GC^* and $\hat{\rho}$ were calculated across 50 kb windows with LOESS curves shown for span of 0.2. (C-D) GC^* and the pseudoautosomal region (PAR). The histogram shows GC^* for chromosome Z across 500 kb windows; GC^* for the 450 kb PAR shown by the vertical line.

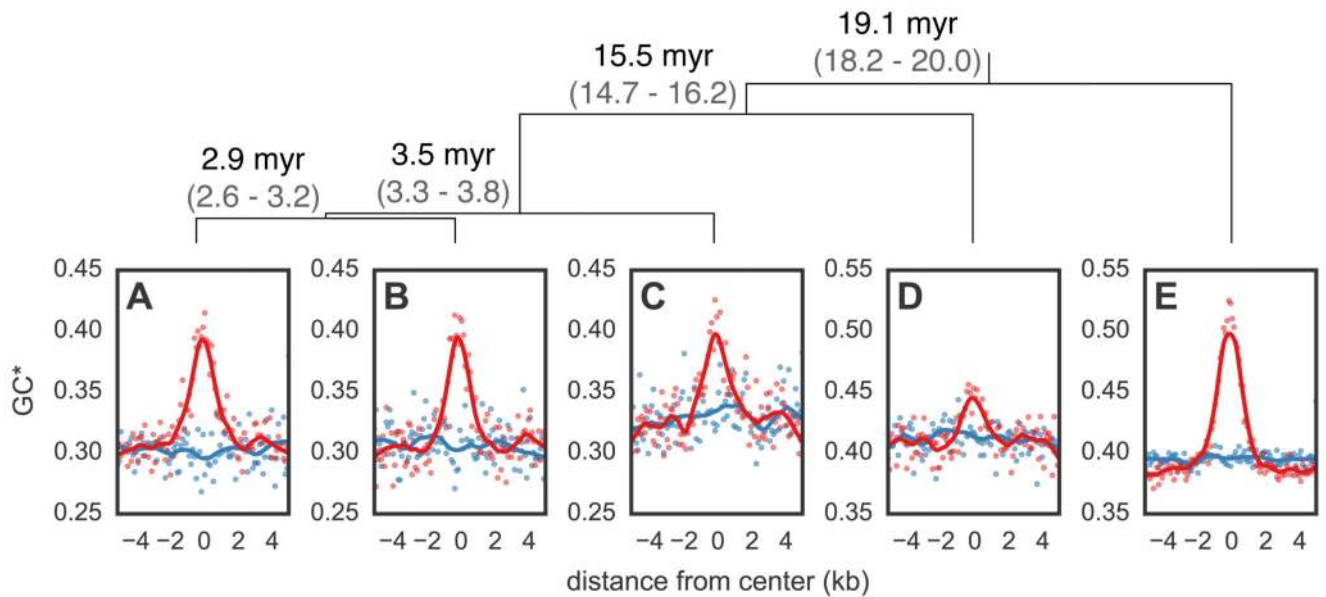


Figure 4.

Expected equilibrium GC content (GC^*) around hotspots and matched coldspots for five bird species. Points (hotspots shown in red and coldspots in blue) represent GC^* estimated from the lineage-specific substitutions aggregated in 100 bp bins from the center of all hotspots in (A) zebra finch and (B) long-tailed finch. GC^* for (C) double-barred finch, (D) medium ground finch, and (E) collared flycatcher was calculated around hotspots identified as shared between zebra finch and long-tailed finch. LOESS curves are shown for a span of 0.2. The orientation of hotspots is with respect to the genomic sequence. Species tree (18) shown with estimated divergence times in millions of years (myr) and its 95% Highest Posterior Density in gray; top.

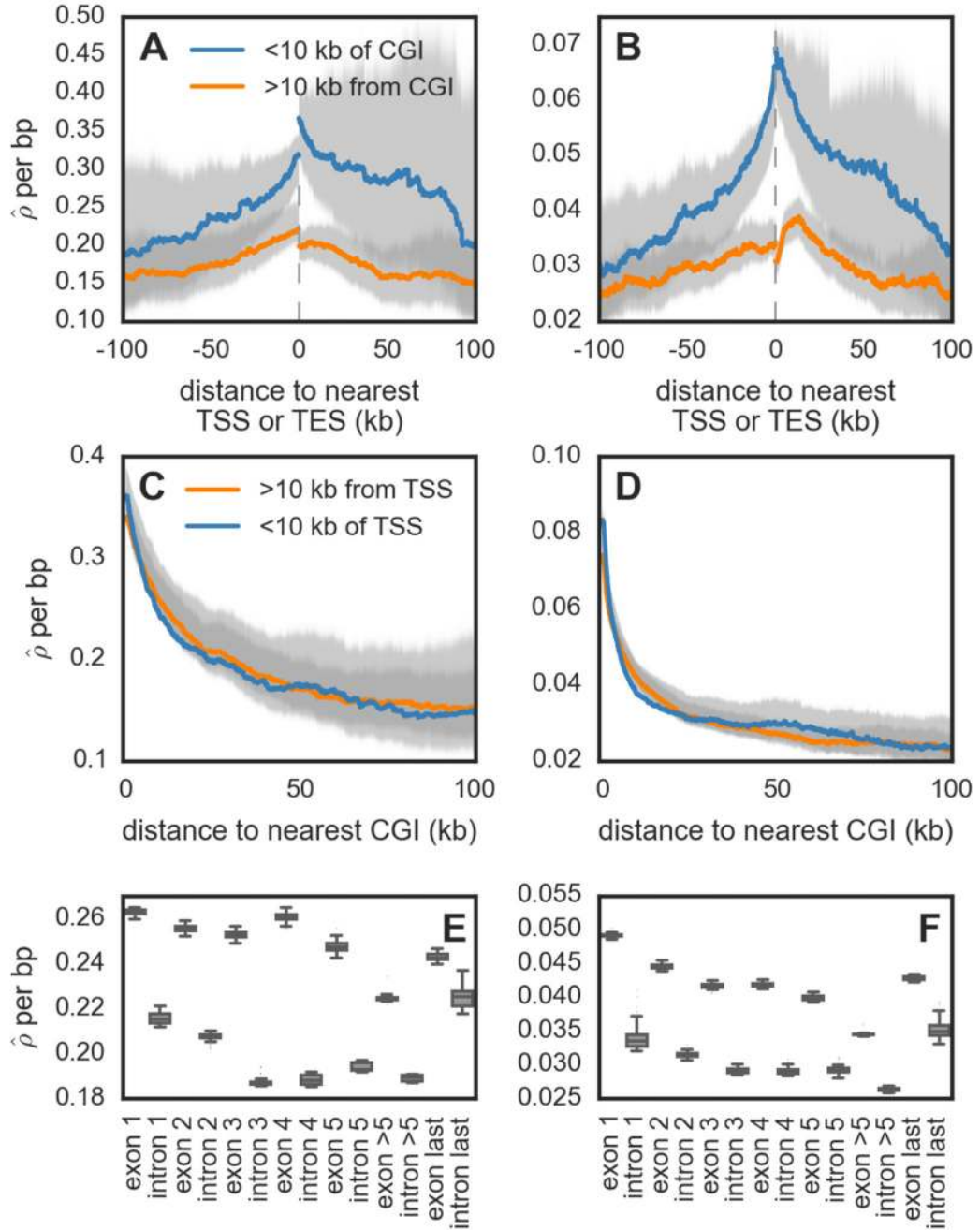


Figure 5.

Recombination rates across genomic features for zebra finch (A, C, E) and long-tailed finch (B, D, F). (A-B) Estimated recombination rates ($\hat{\rho}$ /bp) around annotated transcription start sites (TSSs) and end sites (TESs), conditional on whether they are within 10 kb of a CpG island (CGI) or not. The gray dotted line represents the location of the gene, and the distances are shown accounting for the 5' \rightarrow 3' orientation of genes. (C-D) $\hat{\rho}$ shown as a function of distance to nearest CGI, conditional on whether the CGI is within 10 kb of an annotated TSS or not. See Fig. S17 for the pattern of CGIs relative to TESs. For figures A –

D, uncertainty in rate estimates (shown in gray) was estimated by drawing 100 bootstrap samples and recalculating means. (E-F) \hat{p} within exons and introns for genes that have ≥ 5 exons (n=7,131). See Fig. S28 for simulation results that suggest the inference of higher background \hat{p} in exons does not reflect differences in diversity levels between exons and introns.

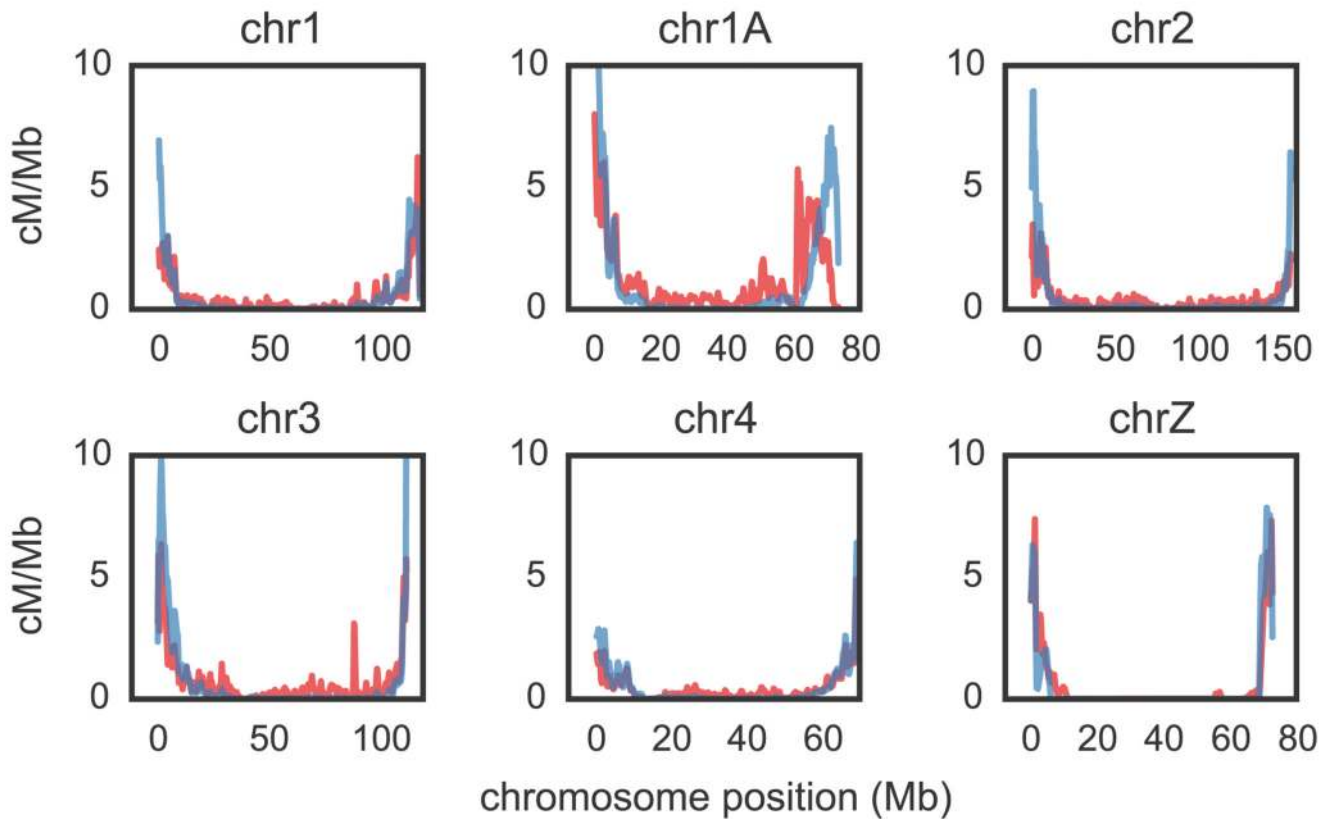


Figure 6.

Comparative recombination rates for zebra finch and long-tailed finch. Zebra finch rates shown in red; long-tailed finch in blue. Estimated rates [cM/Mb; obtained from \hat{p}/bp (18)] are shown as rolling means calculated across 100 kb windows. We show here the five largest autosomal chromosomes and chromosome Z; see Fig. S20 for all chromosomes. Rate estimates for chromosome Z should be taken with caution for both biological and technical reasons (see 18 for more information).